AJNR

Aneurysm Rupture Following Treatment with Flow-Diverting Stents: Computational Hemodynamics Analysis of Treatment

J.R. Cebral, F. Mut, M. Raschi, E. Scrivano, R. Ceratto, P. Lylyk and C.M. Putman

ORIGINAL RESEARCH

J.R. Cebral
F. Mut
M. Raschi
E. Scrivano
R. Ceratto
P. Lylyk
C.M. Putman

Aneurysm Rupture Following Treatment with Flow-Diverting Stents: Computational Hemodynamics Analysis of Treatment

BACKGROUND AND PURPOSE: Flow-diverting approaches to intracranial aneurysm treatment had many promising early results, but recent apparently successful treatments have been complicated by later aneurysm hemorrhage. We analyzed 7 cases of aneurysms treated with flow diversion to explore the possible rupture mechanisms.

MATERIALS AND METHODS: CFD analysis of pre- and posttreatment conditions was performed on 3 giant aneurysms that ruptured after treatment and 4 successfully treated aneurysms. Pre- and posttreatment hemodynamics were compared including WSS, relative blood flows, vascular resistances, and pressures, to identify the effects of flow-diverter placements.

RESULTS: Expected reductions in aneurysm velocity and WSS were obtained, indicating effective flow diversion from the sac into the parent artery, consistent with periprocedural observations. In each case with postaneurysm rupture, the result of flow diversion led to an increase in pressure within the aneurysm. This pressure increase is related to larger effective resistance in the parent artery from placement of the devices and, in 2 cases, the reduction of a preaneurysm stenosis.

CONCLUSIONS: Flow-diversion devices can cause intra-aneurysmal pressure increases, which can potentially lead to rupture, especially for giant aneurysms. This relates both to changes in the parent artery configuration, such as reduction of a proximal stenosis, and to the flow diversion into higher resistance parent artery pathways combined with cerebral autoregulation, leading to higher pressure gradients. These may be important effects that should be considered when planning interventions. Potentially dangerous cases could be identified with angiography and/or patient-specific CFD models.

ABBREVIATIONS: CFD = computational fluid dynamics; ΔP = pressure drop; 3DRA = 3D rotational angiography; ICA = internal carotid artery, PA = parent artery; PED = Pipeline Embolization Device; PTA = percutaneous transarterial angioplasty; Post = after; Pre = before; P_i = pressure at the model inlet; P_o = pressure at the model outlet; P_s = systemic pressure; Q = flow rate; R_a = combined resistance of the aneurysm and the parent artery segment at the aneurysm location; R_d = distal resistance; R_p = proximal resistance; WSS = wall shear stress

The treatment of intracranial aneurysms has gone through dramatic changes with the introduction of interventional techniques. Endosaccular coiling of aneurysms has been shown to be effective and has arguably replaced surgery for the treatment of most aneurysms. However, coiling has significant limitations in achieving durable occlusion of many large and giant aneurysms because of a propensity for recanalization. This problem has largely been the driving force behind the development of flow-diverting devices to treat intracranial aneurysms.[1-3] These devices promote the thrombosis of aneurysms without filling the aneurysm cavity, by deviating the blood flow away from the aneurysm by placing a device solely within the parent artery. Theoretically, this approach would avoid recanalization because the stability of the device within the parent artery maintains a stable long-term hemodynamic environment that is not subject to displacement by the repet-

itive actions of the pulsatile arterial flow. Trials using flow-diverting stents have shown promising initial results in achieving these goals.[4,5] In fact, a total of 217 aneurysms have been successfully treated in 1 such series.[4] However, recent apparently successful treatments have been complicated by later aneurysm hemorrhage, which raises concerns about the safety of this treatment. The purpose of this report was to examine the possible mechanisms responsible for posttreatment ruptures by comparing 3 cases with posttreatment bleeding with 4 aneurysms with successful treatment using flow diversion.

Materials and Methods

Clinical and Imaging Data

Three patents with posttreatment ruptures and 4 patients with successfully treated unruptured aneurysm were studied. All patients were treated with flow-diverting stents, PEDs (ev3, Plymouth, Minnesota). Clinical information is summarized in Table 1. Patients 1 and 3 had narrowed parent arteries. Treatment resulted in opening of the parent artery in these patients. In patient 1, angioplasty was required to achieve full deployment of the stent and resulted in opening of the approximately 50% preaneurysm stenosis. In patient 3, the pretreatment parent artery was significantly tapered at the level of the aneurysm. Placement of the 2 stents led to an enlargement of the parent artery and a more normalized circular cross-section. In each case,

Table 1: Clinical information

| Patient No.	Age (yr)/Sex	Size (mm)	Location	Treatment	Outcome
1	62/F	26	Left ICA superior-hypophyseal	1 PED-associated with 50% stenosis treated with PTA	Ruptured at day 4
2	54/F	25	Right ICA ophthalmic	1 PED	Ruptured intraprocedurally
3	60/F	38	Right ICA ophthalmic	2 PED-restricted PAs opened with stenting	Ruptured at day 7
4	59/F	3.1	Left ICA ophthalmic	1 PED	Complete occlusion at 6 mo
5	39/F	4.6	Right ICA superior-hypophyseal	1 PED	Complete occlusion at 6 mo
6	58/M	9.7	Left ICA cavernous	2 PEDs	Complete occlusion at 12 mo
7	58/F	26	Right ICA ophthalmic	2 PEDs	Complete occlusion at 6 mo
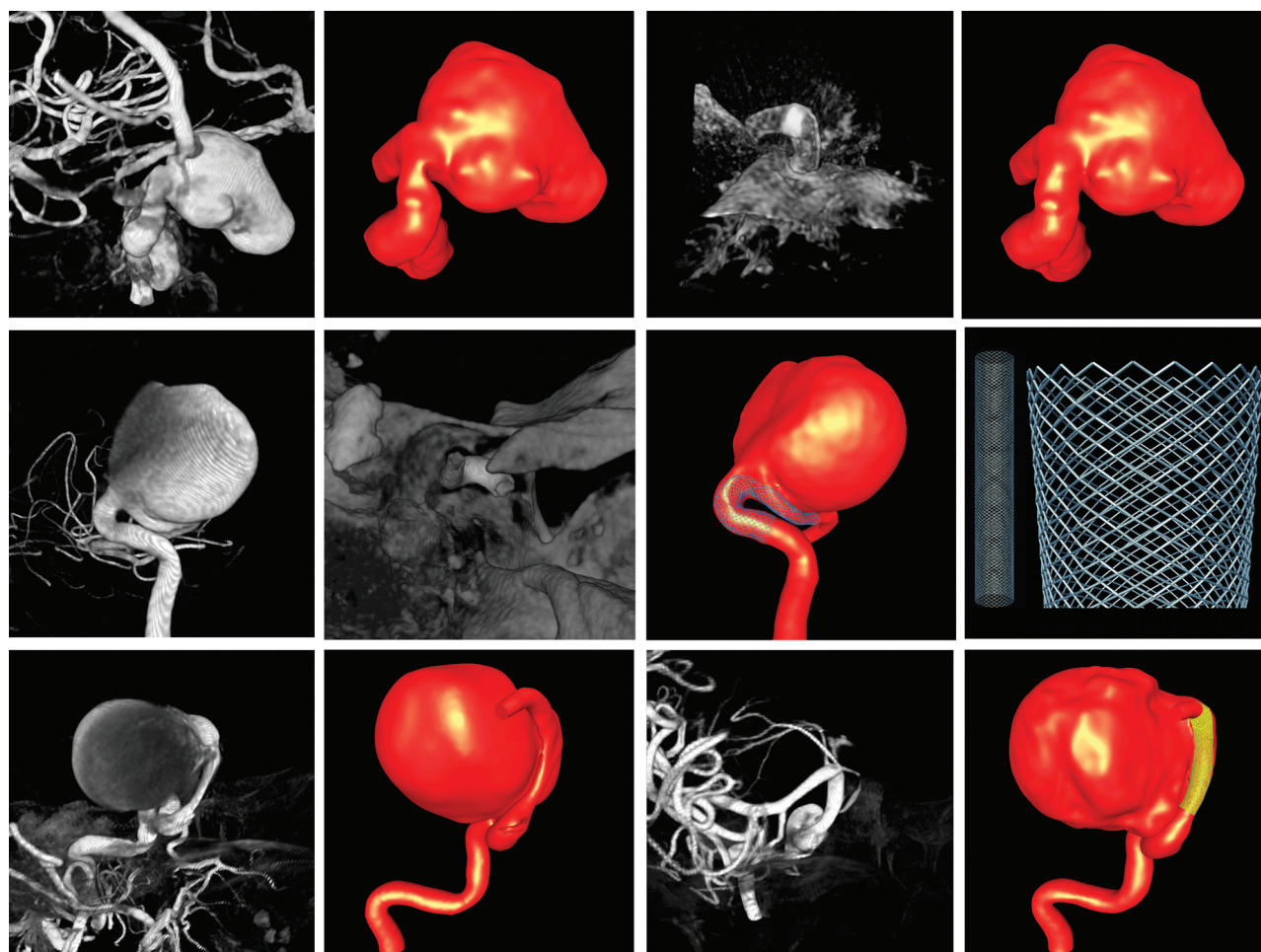
Fig 1. Rotational angiograms prior and immediately after stent placement and corresponding vascular models of 3 aneurysms associated with posttreatment rupture. Top row, patient 1, left to right: 3DRA before treatment, vascular pretreatment model, 3DRA without contrast after stent deployment, and vascular posttreatment model. Center row, patient 2, left to right: 3DRA before treatment, 3DRA without contrast after stent deployment, vascular posttreatment model, and stent design. Bottom row, patient 3, left to right: 3DRA before treatment, vascular pretreatment model, 3DRA after stent placement, and vascular posttreatment model.

posttreatment angiography showed stagnation within the aneurysm with little persistent intra-aneurysmal flow.

Pre- and posttreatment 3DRA images were obtained during a 10-second injection of contrast and a 180° rotation imaging at 15 frames per second for a total of 8 seconds by using an Allura flat panel system (Philips Healthcare, Best, the Netherlands). The projection images were reconstructed on a dedicated Philips XtraVision workstation into 3D datasets of 256 × 256 × 256 isotropic voxels.

Vascular and Stent Models
Computational models of the pre- and poststenting patient-specific vascular geometries were created from the 3DRA images by using a seeded region-growing segmentation, followed by an isosurface de-

formable model.[6] Geometric models of the stents, consisting of 48 wires of 48-μm thickness, were created[7] and placed within the post-stenting vascular models by using a virtual stent-deployment technique.[8] The reference stent diameters were 4 mm (patient 1), 5 mm (patient 2), 3.5 and 4.5 mm (patient 3), 4.5 mm (patient 4), 4.5 mm (patient 5), 5 mm (patient 6), and 4 mm (patient 7). The reconstructed vascular and stent models and the 3DRA images are presented in Figs 1 and 2. To model the effect of the balloon remodeling on the stent of patient 1, we locally modified the stent design at the aneurysm neck, where a lower porosity was observed in the corresponding 3D image. Specifically, the stent cell size in the axial direction was divided by a factor of 6. Unstructured volumetric grids were generated by using an advancing front method and a resolution of
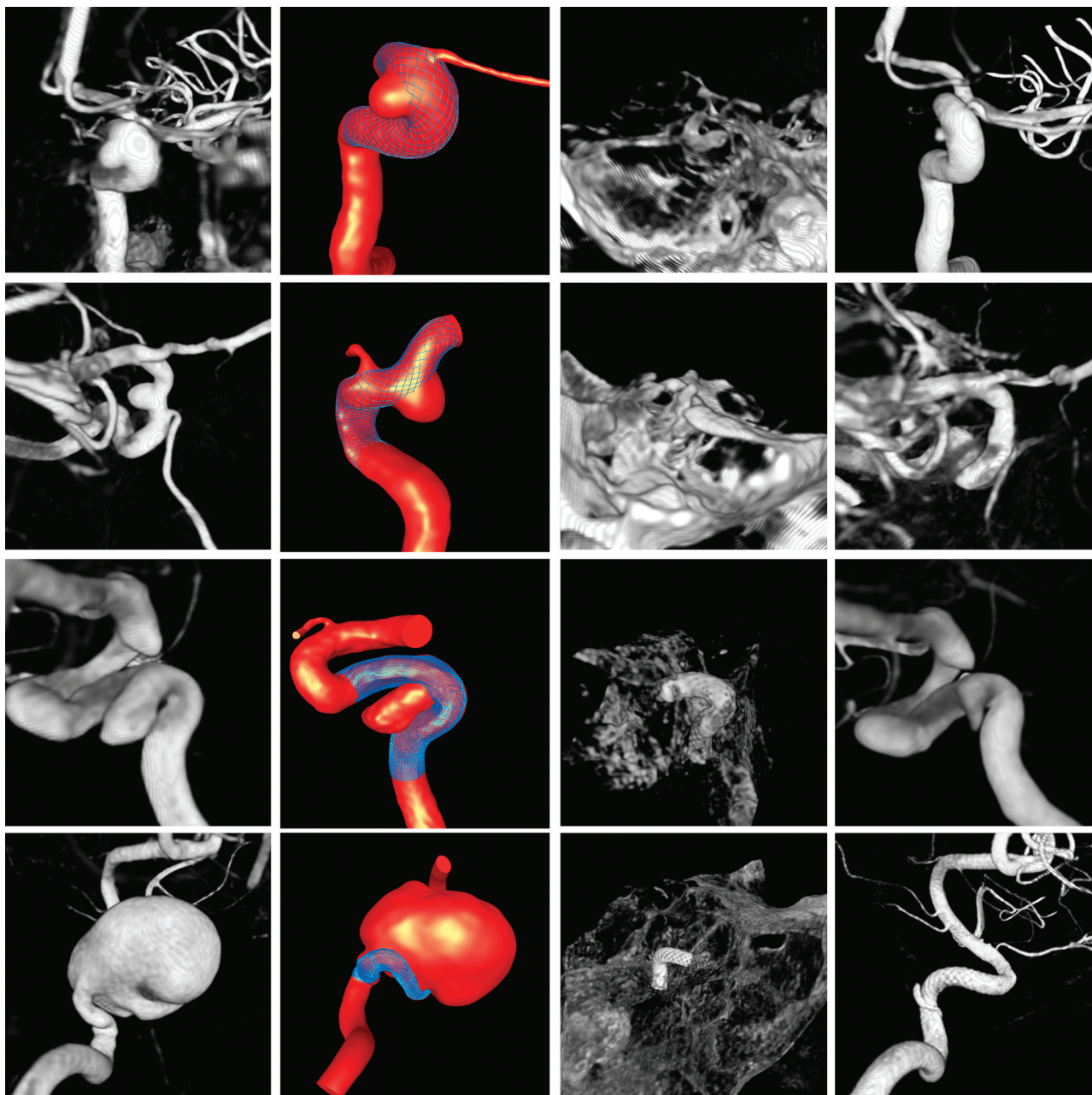
Fig 2. Rotational angiograms and computational models of 4 aneurysms successfully treated with flow diverters. Left to right: 3DRA image before treatment, computational model with stent in place, 3DRA without contrast showing the deployed stents, and follow-up 3DRA images. Rows top to bottom correspond to patients 4–7, respectively.

0.015–0.025 cm,[6] resulting in presenting meshes containing between 600,000 and 6.8 million elements. The poststenting meshes were adaptively refined around the stent wires by using unstructured grid-embedding methods.[9] After 4 levels of mesh adaptation, the final grids contained between 35.2 and 78.1 million elements. Previous studies have shown that these levels of mesh resolution are sufficient for acceptable hemodynamic simulations.[10]

Hemodynamic Models

Blood flows were approximated by the unsteady 3D Navier-Stokes equations for an incompressible Newtonian fluid[11] with an attenuation of $\rho = 1.0 \, \text{g/cm}^3$ and viscosity of $\mu = 0.04$ poise. Vessel walls were assumed rigid, and no-slip boundary conditions were applied at the walls. Because patient-specific flow rates were not available, pulsatile physiologic flow waveforms measured in normal cerebral arteries by using phase-contrast MR imaging were used to impose boundary conditions at the inlets. The flow waveform was scaled with the inlet area to achieve a mean WSS at the inlet of 15 dyne/cm².[12] Corresponding fully developed Womersley profiles were used to prescribe velocity boundary conditions at the inlets.[13] Pressure boundary conditions with P = 0 were applied at the outlets. Identical boundary conditions and model parameters were used in the pre- and poststent placement models. The governing equations were solved by using a fully implicit finite-element formulation and a deflated conjugate gradient algorithm to accelerate the convergence of the pressure Poisson equation at each time-step.[14] Unstructured embedded grid methods were used to solve the governing equations for the poststenting models.[10] The CFD simulations were run for 2 cardiac cycles with a time-step of 0.01 seconds. Results are presented for the second cycle. To estimate the change in the intra-aneurysmal pressures, we as-
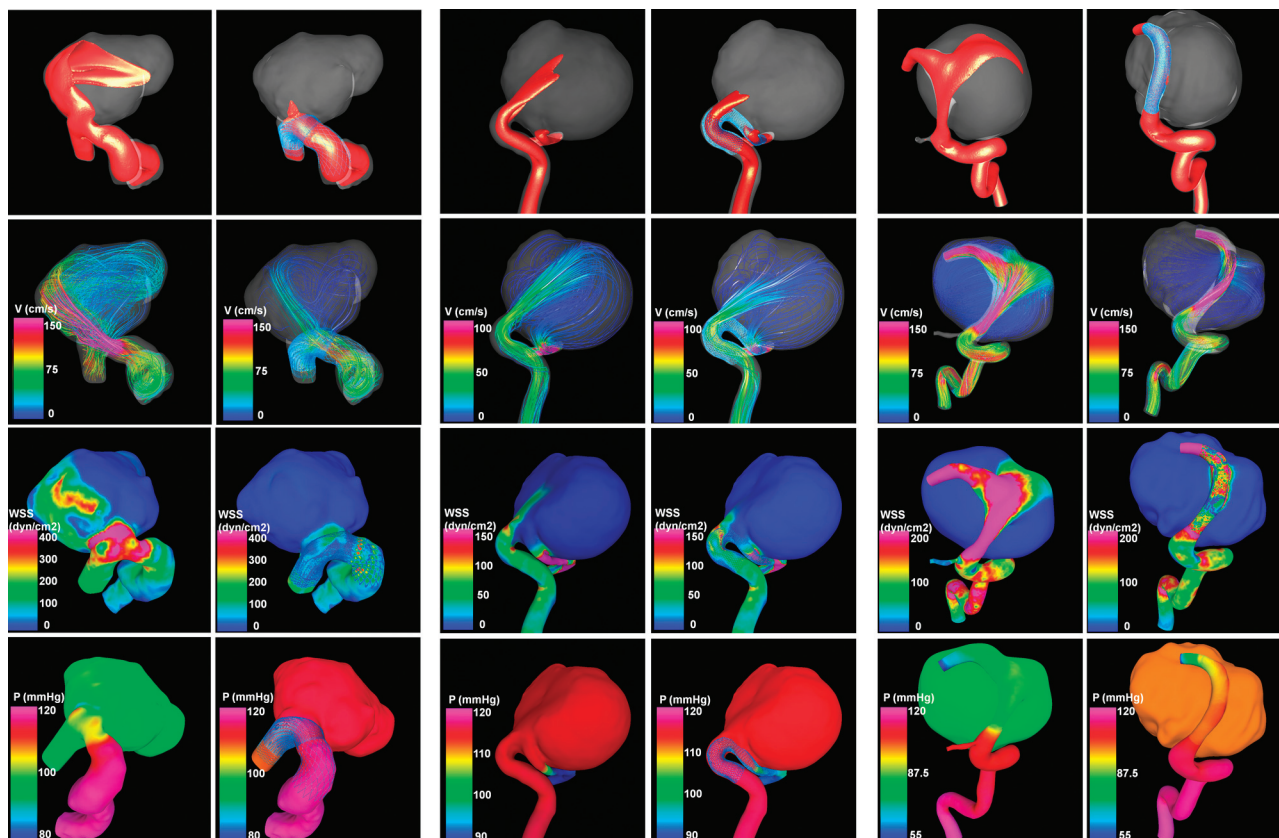
Fig 3. Visualizations of the hemodynamics of patients 1–3 at peak systole before (left column) and after (right column) stent placement. Top to bottom: isovelocity surfaces, velocity color-coded streamlines, WSS distribution, and pressure distributions.

Fig 4. Visualizations of the hemodynamics of patients 4–7 at peak systole before (left column) and after (right column) stent placement. Top to bottom: isovelocity surfaces, velocity color-coded streamlines, WSS distribution, and pressure distributions.
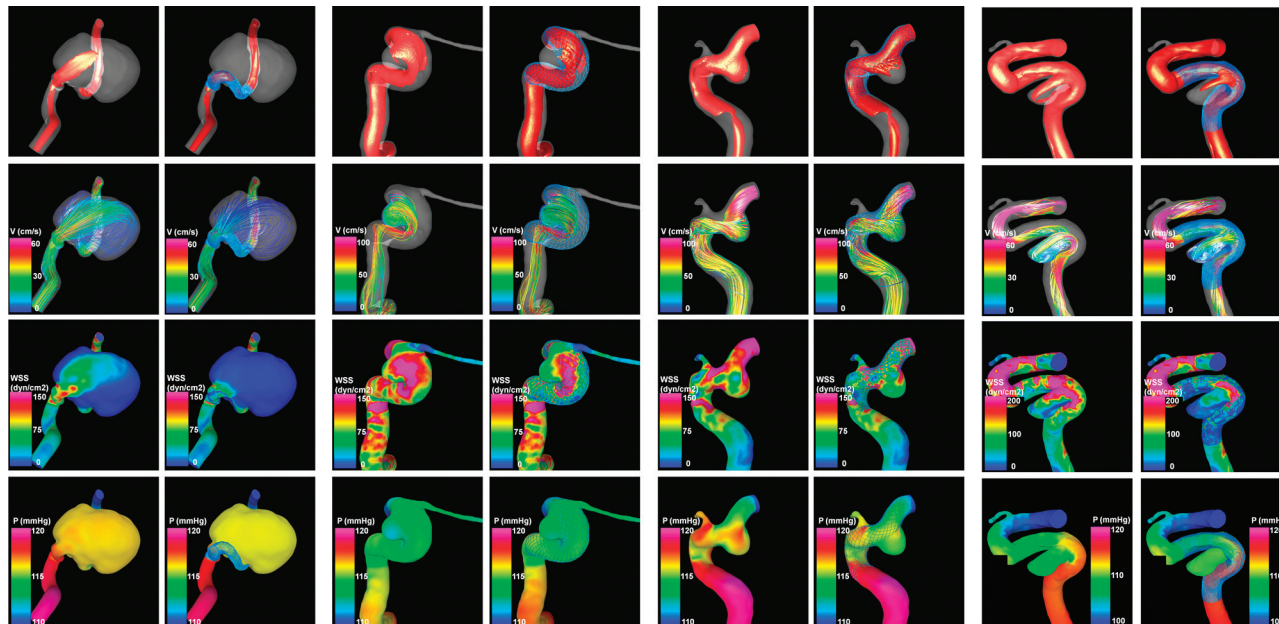
sumed that at the inlets, the intra-arterial pressure at peak systole was 120 mm Hg, both before and after stent placement. Then, the pressure distribution along the parent artery and in the aneurysm was computed by using the pressure drops calculated during the CFD simulations with respect to the P = 0 value prescribed at the outlet.

Results

Visualizations of the results corresponding to patients 1–3 are presented in Fig 3 and to patients 4–7, in Fig 4. These figures show, from top to bottom, peak systole visualizations of the following: 1) the blood flow stream entering the aneurysms by

Table 2: Pressures, resistances, and flow rates corresponding to the electric circuit analog of patient 2 (Fig 5)

Case	P_s (mm Hg)	P_i (mm Hg)	P_o (mm Hg)	R_p (dyne/s/cm⁵)	R_d (dyne/s/cm⁵)	R_a (dyne/s/cm⁵)	Q (mL/s)	ΔP (mm Hg)
Pre	120	110	100	5800	57,900	5800	2.30	–
Post	120	112	72	5800	55,000	23,200	1.90	2
	125	117	77	5800	55,000	23,200	1.98	7
	130	122	81	5800	55,000	23,200	2.06	12
	135	126	86	5800	55,000	23,200	2.15	16
	140	130	90	5800	55,000	23,200	2.22	20
	145	135	95	5800	55,000	23,200	2.30	25

using isovelocity surfaces corresponding to 50 cm/s, 2) the blood flow patterns by using streamlines color-coded with the velocity magnitude, 3) the distributions of WSS, and 4) the pressure distributions. Each panel corresponds to a different patient, and the left and right columns of each panel correspond to the hemodynamics before and after stent placement, respectively.

In all cases, blood streams into the aneurysm and results in regions of elevated WSS in the aneurysm body or dome. After flow-diverter placement, most of the flow stream is diverted through the parent artery with only a small residual flow into the aneurysm. This results in a substantial reduction in overall WSS, a dispersion of focal regions of elevated WSS, and a slow intra-aneurysmal circulation.

In the cases associated with posttreatment rupture (patients 1–3), there is an elevated pressure gradient across the aneurysm segment. Following flow-diverter placement, pressure drops in the aneurysm segment are reduced, causing an increase in intra-aneurysmal pressure. In patient 1, the preaneurysm stenosis was opened; this change reduced the pressure drop from 25 mm Hg to 5 mm Hg. As a consequence, the intra-aneurysmal pressure was increased by 20 mm Hg.

In patient 2, flow was redirected from primarily entering the aneurysm through the more confined pathway through the parent artery. This path was characterized by a sharp bend near the proximal end of the neck and a substantial tapering from the proximal to the distal ends of the stent. This resulted in an elevated pressure drop along the treated segment to approximately 40 mm Hg at peak systole. This increased pressure drop reflected an increased flow resistance of this segment. Using the assumption that the proximal resistance does not change after stent placement and that the distal resistance can only diminish by approximately 5% due to autoregulation of the distal vascular bed, we calculated the flow rate and the corresponding inlet and outlet pressures for different systemic pressures. The results are presented in Table 2. If one assumes that the systemic pressure is maintained after stent placement, the flow rate through the aneurysmal arterial segment will decrease by approximately 20%. This flow rate will produce a smaller pressure drop in the proximal artery; thus, the intra-aneurysmal pressure should increase by approximately 2 mm Hg. If the systemic pressure increases to maintain the flow, the intra-aneurysmal flow can increase up to approximately 25 mmHg, compared with the pretreatment state.

In patient 3, before treatment, the blood flow in the proximal segment of the parent artery accelerated as the artery cross-sectional area decreased. This resulted in a pressure drop along the parent artery from the proximal part to the aneurysm orifice of approximately 45 mm Hg at peak systole. Most of the blood flow from the parent artery then entered the an-

eurysm, impacting the distal part of the aneurysm body and dispersing into a complex flow structure. After stent placement, the proximal parent artery diameter was enlarged and the cross-sections became more circular. This resulted in a decreased pressure drop to approximately 20 mm Hg along the proximal segment. The flow stream was almost completely redirected away from the aneurysm, but it was forced to follow a relatively sharp turn immediately distal of the aneurysm neck, which causesd an increased pressure drop at this location. The combination of these 2 effects resulted in a total pressure drop from the inlet to the outlet, very similar to that of the prestenting model. However, the pressure in the aneurysm increased by approximately 25 mm Hg.

In the cases not associated with posttreatment rupture (patients 4–7), parent artery effects and flow stream paths did not result in substantial gradients across the aneurysm segment. Placement of the flow-diverting stent did not result in any substantial alterations of the intra-aneurysmal pressures (<3 mm Hg for all 4 cases).

Discussion

Development of new hemodynamic approaches to the treatment of intracranial aneurysms is a major departure from the traditional therapies. Rather than mechanically excluding the aneurysm sac from the circulation, this approach targets a reconstruction of the normal hemodynamics of the parent artery. Placement of the flow-diverting device within the parent artery and across the orifice of the aneurysm creates a redirection of flow through the parent artery and establishes a low-flow hemodynamic state within the aneurysm that would favor its thrombosis and ultimate occlusion and remodeling.[15] Because of the inherent stability of the endoluminal device, this approach potentially avoids the subsequent compaction often seen in endosaccular coiling approaches resulting in aneurysm recurrence. Given the high recurrence rates seen in coiling of large wide-neck aneurysms, flow-diverting approaches appear to be an attractive treatment option for these aneurysms. However, there are several potential drawbacks. First, the flow diverter does not mechanically exclude the aneurysm from the flow stream but relies on the hemodynamic environment created to initiate thrombosis and remodeling, to ultimately seal the aneurysm. This process takes time, so the immediate elimination of the aneurysm cannot be expected. Until the healing of the aneurysm has been completed, the aneurysm wall is subject to the stresses and strains imposed by the pulsatile arterial circulation. Furthermore, the aneurysm wall is subject to the biologic processes related to the local thrombosis, which may initially be potentially damaging. A reduction of flow does not equate to a reduction of the pressures experienced by the aneurysm wall, leaving a potentially

dangerous period of time when an as-yet-unreinforced aneurysm and potentially even the weakening wall may be subject to adversely altered hemodynamics. Second, the placement of the flow-diverting device blocks access to the aneurysm sac, limiting endovascular options in situations of a treatment failure or aneurysm recurrence.

Trials by using flow-diverting stents have shown promising initial results in achieving occlusion of large and giant aneurysms[4]; however, recent apparently successful treatments have been complicated by later aneurysm hemorrhage. We have used patient-specific hemodynamic analysis of 3 cases in which posttreatment rupture occurred and 4 cases of successful treatment to examine the hemodynamic changes that may be responsible for the treatment failures. In all cases, our simulations identified the expected reductions in flow velocity and WSS within the aneurysm, indicating the effective flow diversion from the aneurysm sac into the parent artery. These results are consistent with observations made during the endovascular intervention that little or no contrast entered the aneurysm after treatment. However, in each case associated with posttreatment rupture, according to the CFD calculations, the result of flow diversion led to an increase in pressure within the aneurysm sac in contrast to the 4 other successful treatment cases in which no substantial increase in pressure was observed. Posttreatment elevation of the intra-aneurysmal pressure would increase the stress on the aneurysm wall. Because this effect is immediate and the reparative mechanisms responsible for the aneurysm healing take time, there is a potential period of increased risk of aneurysm rupture until the aneurysm thrombosis has occurred. Presumably, if the aneurysm wall is very weak, a relatively small pressure increase could cause its rupture. If aneurysm size is assumed to be a good indicator of wall weakness, it is to be expected that large and giant aneurysms would be more vulnerable to this effect. In fact, in this study, all 3 cases associated with posttreatment bleeds involved giant aneurysms, suggesting that indeed the aneurysm wall may have been very weak and close to its rupture.

The numeric simulations point to 2 possible explanations for the increased intra-aneurysmal pressure after flow-diverter placement. In 2 of the cases, the parent artery initially contained a focal segment of moderate stenosis. This stenosis was opened by angioplasty in 1 case and by placement of 2 stents in the second, to achieve appropriate deployment of the flow-diverter device. In both cases, the enlargement of the vessel lumen was a consequence of the maneuvers carried out to properly appose the stents. The treatment did not specifically target the stenoses. Reduction in this proximal resistance led to increased flow into the aneurysm segment and a subsequent increase in intra-aneurysmal pressure. This effect is well known by endovascular specialists and is readily understandable.

The second effect of placement of the flow diverter is more difficult to explain. The placement of the flow diverter results in an increased resistance in the aneurysm segment. Before treatment, the flow stream has 2 paths for flow, into the aneurysm and along the parent artery. This is effectively 2 resistors in parallel as can be illustrated in a simple electric circuit analogy shown in Fig 5. Placement of the flow diverter leads to a concentration of the flow through the parent artery, a more
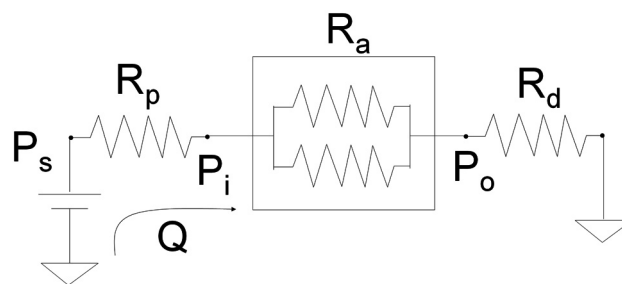

Fig 5. Electric circuit analog.

confined space, and forces the flow into the higher resistance pathway. Therefore, the total resistance of the flow in the aneurysm segment is increased. If systemic pressures remain constant post–stent placement, then flow rates within the aneurysm segment will decrease by approximately 20%, which will result in a modest pressure drop and an increase of intra-aneurysmal pressure of only approximately 2 mm Hg.

However, the complex system of autoregulation in the cerebral vascular circulation works to maintain cerebral perfusion. Although collateral circulation may make up for this increase in cerebral blood flow in some patients, the autoregulation mechanisms will, in part, work to maintain the flow. So, increasing the resistance locally would result in a reduction in distal vascular resistance, and systemic blood pressure may increase to maintain flow. As the flow rate increases in the aneurysm segment, the effect on intra-aneurysmal pressure is increased as demonstrated by the calculations reported in Table 1. With relatively small elevations in systemic pressure, substantial increases in intra-aneurysmal pressure can be found. If the flow is returned to the pretreatment level, then pressure in the aneurysm can increase to as much as 25 mm Hg.

Our analysis raises concern over a potential period when aneurysm wall tensions are increased after placement of a flow diverter before the processes of thrombosis and remodeling ultimately strengthen the aneurysm wall. Knowledge of these hemodynamic effects can be useful for the planning of endovascular therapies using flow diverters. Two features that may place an aneurysm at increased risk for posttreatment rupture can be identified before treatment. First, aneurysms arising from arteries with a stenosis proximal to the aneurysm orifice have the potential for increased intra-aneurysmal pressure if the flow diverter placement results in opening of the stenosis. Second, aneurysms that accept most of the parent artery flow (usually associated with severe parent artery tortuosity) may have a rise in local resistance following placement of a flow diverter, particularly in large and giant aneurysms. Autoregulation acting to maintain flow may result in a rise in the pressure gradient and a rise in the intra-aneurysmal pressure. These aneurysms could be readily identified before treatment through CFD analysis.

Although some of these models are still computationally intensive, typically treatments are considered for elective patients with geometrically complex unruptured aneurysms that are difficult to coil or clip. For this subset of patients, there is enough time to perform CFD analyses to plan and evaluate the interventions. When CFD is not readily available, high-frame-rate angiography can be performed to visualize the inflow

stream, so that a basic assessment of how the relative flow into the aneurysm compares with that of the parent artery stream,[16] allowing identification of these potentially high-risk situations. Additionally, if stenoses are observed during angiographic examinations, the associated pressure drops could also be roughly estimated by using simple formulas.

Our analysis also suggests some measures that can be undertaken by the endovascular specialist to help mitigate this pressure increase. A modest reduction in systemic blood pressure can minimize any elevations of intra-aneurysmal pressures. Careful blood pressure control in the posttreatment period could be a practical method of minimizing posttreatment rupture. To minimize the time period for risk in the posttreatment window, methods of more rapidly achieving aneurysm thrombosis should be considered. Placement of a coil or other prothrombotic devices in the aneurysm sac before the deployment of the flow diverter could meet this goal. Placement of multiple flow diverters within a single patient could speed the progression of thrombosis but is not without a drawback. Multiple flow diverters would reduce flow into the aneurysm but would also increase the effective resistance in the aneurysm segment and, consequently, may lead to a potentially greater rise in intra-aneurysmal pressure.

The current study highlights an important hemodynamic effect (intra-aneurysmal pressure increase) that may be the cause of the subsequent rupture of the aneurysm. However, further analysis of a larger series of treated aneurysms will be necessary before drawing any definitive conclusions. This study only provides information about the hemodynamic environment of the aneurysms just before rupture. Unfortunately, no other information (including pathology) was available to complement or confirm these observations and help us to better understand the underlying mechanism leading to rupture. In particular, we do not have any information regarding the intra-aneurysmal clot and its evolution in the aneurysmal hemodynamic environment. There may have been other mechanisms at play that caused the ruptures—for instance, inflammation induced by the low-flow state near the aneurysm wall, possible damage of the artery wall during the endovascular therapy, or perhaps even more complex multifactorial processes.

The current study has several limitations common to most CFD hemodynamic analyses that should be considered when evaluating the results. These include the following: the assumption of rigid walls, physiologic but not patient-specific flow-boundary conditions, Newtonian blood properties, and limited mesh and time-step resolutions. Rigid-walled CFD models can overestimate pressure gradients; thus, the pressure increases obtained may be larger than in reality. Additionally, the exact geometry of the stent in its deployed state and after balloon remodeling was unknown and was approximated. Despite these limitations, the observation that the removal of a proximal stenosis and placement of a flow-diverting device

may cause an increase in the intra-aneurysmal pressure and may have a potentially adverse effect on the aneurysm is important to consider when planning interventions with these devices.

Conclusions
Placement of a flow-diversion device can increase in the intra-aneurysmal pressure, which can potentially cause the rupture of the aneurysm, especially giant aneurysms that may have very weak walls. This relates both to the inherent flow diversion into the higher resistance parent artery pathway in combination with cerebral autoregulation leading to higher pressure gradients and to changes in the parent artery configuration such as reduction of a proximal parent artery stenosis. This may be an important effect that should be considered when planning endovascular interventions with flow-diverting devices. Potentially dangerous cases in which significant pressure drops are expected could be identified with angiography and/or patient-specific CFD models.

References
1. Lylyk P, Ferrario A, Pasbon B, et al. **Buenos Aires experience with the Neuroform self-expanding stent for the treatment of intracranial aneurysms.** *J Neurosurg* 2005;102:235–41
2. Lövblad KO, Yilmaz H, Chouiter A, et al. **Intracranial aneurysm stenting: follow-up with MR angiography.** *J Magn Reson Imaging* 2006;24:418–22
3. Szikora I, Berentei Z, Kulcsar Z, et al. **Endovascular treatment of intracranial aneurysms with parent vessel reconstruction using balloon and self-expandable stents.** *Acta Neurichir* 2006;148:711–23, discussion 723. Epub 2006 May 17
4. Lylyk P, Miranda C, Ceratto R, et al. **Curative endovascular reconstruction of cerebral aneurysms with the Pipeline embolization device: the Buenos Aires experience.** *Neurosurgery* 2009;64:632–42
5. Szikora I, Berentei Z, Kulcsar Z, et al. **Treatment of intracranial aneurysms by functional reconstruction of the parent artery: the Budapest experience with the Pipeline embolization device.** *AJNR Am J Neuroradiol* 2010;31:1139–47. Epub 2010 Feb 11
6. Cebral JR, Castro MA, Appanaboyina S, et al. **Efficient pipeline for image-based patient-specific analysis of cerebral aneurysm hemodynamics: technique and sensitivity.** *IEEE Trans Med Imaging* 2005;24:457–67
7. Kallmes DF, Ding YH, Dai D, et al. **A new endoluminal, flow disrupting device for treatment of saccular aneurysms.** *Stroke* 2007;38:2346–52
8. Mut F, Appanaboyina S, Cebral JR. **Simulation of stent deployment in patient-specific cerebral aneurysm models for their hemodynamics analysis.** In: *Proceedings of the Summer Bioengineering Conference of the American Society of Mechanical Engineers,* Marco Island, Florida. June 25–29, 2008
9. Cebral JR, Löhner R. **Efficient simulation of blood flow past complex endovascular devices using an adaptive embedding technique.** *IEEE Trans Med Imaging* 2005;24:468–77
10. Appanaboyina S, Mut F, Löhner R, et al. **Computational fluid dynamics of stented intracranial aneurysms using adaptive embedded unstructured grids.** *Int J Numer Meth Fluids* 2008;57:457–93
11. Kundu PK, Cohen IM. *Fluid Mechanics.* New York: Academic Press (Elsevier); 2004
12. Cebral JR, Castro MA, Putman CM, et al. **Flow-area relationship in internal carotid and vertebral arteries.** *Physiol Meas* 2008;29:585–94
13. Taylor CA, Hughes TJR, Zarins CK. **Finite element modeling of blood flow in arteries.** *Comp Methods Appl Mech Eng* 1998;158:155–96
14. Mut F, Aubry R, Löhner R, et al. **Fast numerical solutions in patient-specific simulations of arterial models.** *Int J Num Meth Biomed Eng* 2010;26:73–85
15. Lieber BB, Stancampiano AP, Wakhloo AK. **Alteration of hemodynamics in aneurysm models by stenting: influence of stent porosity.** *Ann Biomed Eng* 1997;25:460–69
16. Cebral JR, Pergolizzi R, Putman CM. **Computational fluid dynamics modeling of intracranial aneurysms: qualitative comparison with cerebral angiography.** *Acad Radiol* 2007;14:804–13